Electronic supplementary information

Design of textured multi-layered structures via magnetically assisted slip casting

Hortense Le Ferrand, Florian Bouville*, André R. Studart*

Complex Materials, Department of Materials, ETH Zurich, 8093 Zurich, Switzerland

*f.bouville@imperial.ac.uk, *andre.studart@mat.ethz.ch

Supplementary Figures

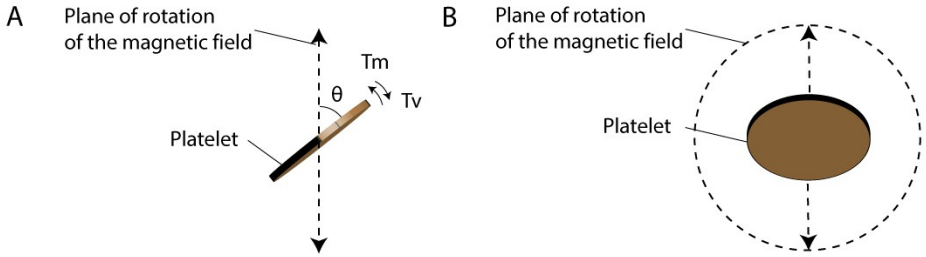

Supplementary Figure 1: Platelet submitted to a rotating magnetic field: **A**) View orthogonal to the plane of the rotating magnetic field. **B**) View onto the plane of the field.

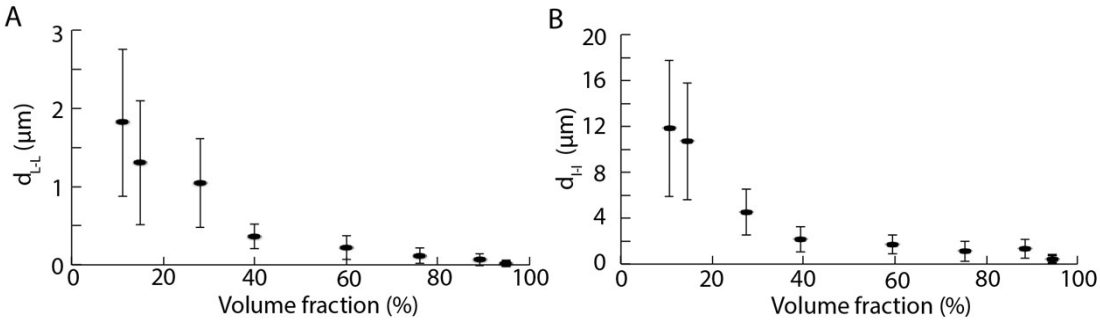

Supplementary Figure 2: A,B) Experimental values of the interplatelet distances for the particles of aspect ratio 30.

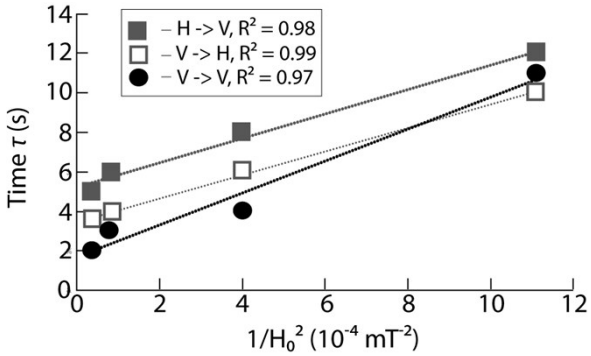

Supplementary Figure 3: Alignment time τ as a function of $\frac{1}{H_0^2}$. The lines correspond to a linear fit of equation 1 (main text) to the experimental data. The slopes of each line correspond to the constant C_1 and are equal to 6200, 5949 and 8117 $\cdot 10^{-4}\, s.mT^2$ for the transitions H->V, V->H and V->V, respectively.

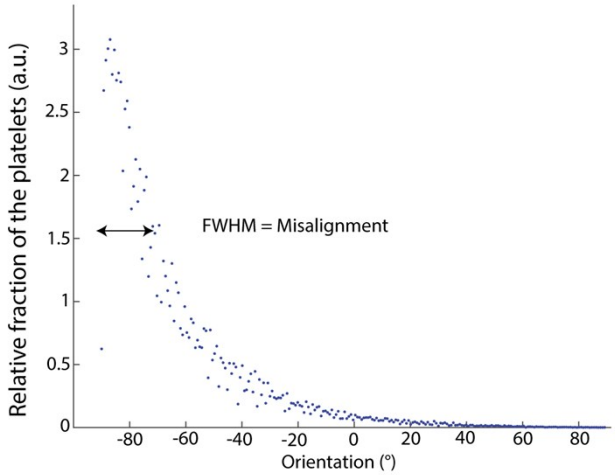

Supplementary Figure 4: Angle distribution of the platelet orientation in a vertically aligned sample containing 25 vol% of platelets. The Full Width at Half Maximum (FWHM) represents the degree of misalignment of the vertical platelets.

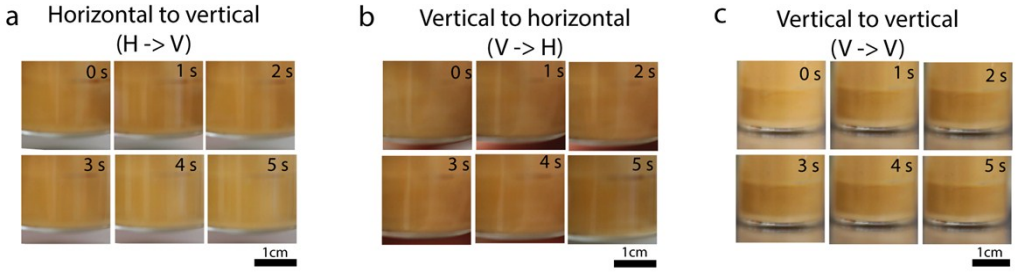

Supplementary Figure 5: Snapshots of suspensions containing 25 vol% platelets in 5 wt% PVP aqueous solution and subjected to a magnetic field strength H_0 = 165 mT rotating at 1 Hz. Image series (**a**-**c**) show the colour change with time for distinct alignment scenarios.

Supplementary text

Physical forces and torques relevant for the MASC process

Gravitational, viscous and magnetic torques

Assuming an isolated platelet suspended in a continuous fluid medium, the gravitational, magnetic and viscous torques exerted at the edge of the platelet under and external magnetic field can be expressed as [21]:

$$T_g = 2\pi\rho ab^3 g cos\phi_p, \quad \text{(Eq. S1)}$$

$$T_m = \frac{2\pi\mu_0\chi_{ps}^2}{3(\chi_{ps}+1)}\left[(a+d)(b+d)^2 - ab^2\right]H_0^2(t)sin(2\theta) \quad \text{(Eq. S2)}$$

and

$$T_v = -6\eta V\left(\frac{f}{f_0}\right)\left(\frac{d\phi_p}{dt}\right) \quad \text{(Eq. S3)}$$

where ρ is the density mismatch between the platelets and the surrounding fluid, ϕ_p is the angle between the platelet's long axis and the substrate, $\theta = \phi_m - \phi_p$, ϕ_m the angle of the magnetic alignment direction and the substrate, *g* is the gravitational constant, η is the viscosity of the surrounding Newtonian fluid, *V* is the volume of the platelet given by $V = 2\pi ab^2$, *a* and *b* are half the thickness and half the diameter of the platelet, respectively; *d* is the thickness of the magnetic shell coating the platelets, f/f_0 is the Perrin friction factor given by

$$\frac{f}{f_0} = \frac{4(1-p^2)}{3(2-p^2aS)}$$

p is the aspect ratio of the platelets (*b/a*),

$$S = \left(\frac{2}{a}\right)(p^2-1)^{-1/2}tan^{-1}\left[(p^2-1)^{1/2}\right],$$

μ_0 is the magnetic permeability of free space, and χ_{ps} is the magnetic susceptibility of the particle shell (**Table 1**).

Table 1: Input data used to calculate the torques

a	$1.5 \cdot 10^{-7}$	m
b	$5 \cdot 10^{-6}$	m
d	$1.2 \cdot 10^{-8}$	m
H_0	$3.99 \cdot 10^{6}$	A/m
χ_{ps}	1.33 (Ref 13)	-

μ_0	$1.26 \cdot 10^{-6}$	Kg.m.s^{-2}
g	10	m.s^{-2}
ρ	2200	Kg.m^{-3}
η	$1.83 \cdot 10^{-2}$	Kg.m^{-1}s^{-2}
$\frac{f}{f_0}$	16.5	-

Hydrodynamic torque

For a platelet positioned close to the wall of the mould, local fluid flow induces a drag force and an associated hydrodynamic torque, T_h. The hydrodynamic torque depends on the local shear rate and can induce orbital motion of the platelets, known as Jeffery orbits[29,30]. The local shear rate depends on the volumetric flow rate, Q. The flow rate close to the wall decreases with the increase in deposit layer thickness due to the resistance of the newly formed jammed layer against flow into the mould.[31] This correlation can be expressed by[19,39] :

$$|Q(t)| = |V| = \frac{S}{J}\left|\frac{dx}{dt}\right| \quad \text{(Eq. S4)}$$

where S is the surface area of the substrate, x is the thickness of the deposit layer and J is the ratio between the volume of the deposited layer and the volume of extracted liquid. Taking υ_i as the volume fraction of particles in the initial suspension and υ_d as the volume fraction of particles in the deposited layer, the J value is given by: $J = \frac{\upsilon_i}{\upsilon_d - \upsilon_i}$.

To estimate the hydrodynamic torque, we consider the cylindrical geometry of our mould, which is comprised of a vertical plastic tube glued on top of a gypsum substrate. For this geometry and similar suspensions to the ones used in this study, we have previously observed that the growth of the deposit as a function of time can be described by the relation[15]:

$$x(t) = \alpha\sqrt{t} \quad \text{(Eq. S5)}$$

where α is a constant that depends on the particle concentration, the hydrostatic resistance δ, the capillary pressure Δp at the pores of the mold and the fluid viscosity as follows:

$$\alpha = \sqrt{\frac{2J\Delta p}{\eta\delta}}$$

Introducing Eq. S5 into Eq. S4 we obtain:

$$|Q(t)| = \frac{\pi R^2}{J}|\dot{x}| = \frac{\pi R^2\,\alpha}{2J\,\sqrt{t}} = \frac{\pi R^2\alpha^2}{2J\;\;x} \quad \text{(Eq. S6)}$$

where R is the diameter of the cylindrical casting tube.

Assuming a shear rate profile generated by flow in a pipe of circular cross-section, the maximum hydrodynamic torque experienced by the platelets is given by[29,30]

$$T_h = \frac{8\pi L^3 \frac{f}{f_0}}{3\ln(2s)} \eta \frac{16}{\pi R^4} Q \quad \text{(Eq. S7)}$$

where *L=2b* is the platelet long-axis length. This relation applies to isolated platelets in a shear gradient and thus neglects inter-particle interactions.

Although we have no experimental evidence that pipe flow conditions are valid for our casting geometry, we use equation S7 to obtain an order of magnitude estimate of the hydrodynamic torques that could potentially develop in our process.

To this end, equations S7 and S6 are combined to obtain the maximum hydrodynamic torque experienced by the platelets as a function of the thickness *x* of the deposit:

$$T_h = \frac{8\pi L^3 \frac{f}{f_0}}{3\ln(2s)} \eta \frac{16\ \pi R^2 \alpha^2}{\pi R^4\ 2J\ \ x} = \frac{8\pi L^3 \frac{f}{f_0}}{3\ln(2s)} \eta \frac{8\ \alpha^2}{JR^2\ x} \quad \text{(Eq. S8)}$$

This theoretical expression shows that the hydrodynamic drag torque scales with the inverse of the deposit layer thickness. We estimate the magnitude of this torque using α = 0.534 mm.s$^{-0.5}$ determined in our earlier work on similar suspensions of platelets.[15] *R* and *J* values of 5 mm and 1.25 were also used in the calculation based on the dimensions of the casting cylinder and on experimentally measured values of v_i and v_d, respectively. Our analysis indicates that the hydrodynamic torque dominates the platelet orientation in the region close to the surface of the substrate but becomes negligible above a critical deposit thickness (**Figure 5**, main text).[39] This is likely the reason for the observed horizontal orientation of platelets only close to the surface of the gypsum substrate.

Capillary torque

Drying of the deposit layer generates a capillary torque on the platelets due to the formation of a liquid meniscus. Such torque is directed towards the mould's surface and can be quantified by estimating the Laplace pressure associated with the meniscus. The level of capillary torque generated depends whether the system is modelled as an isolated meniscus bridge between two vertical particles or as vertical particles partially immersed in the liquid. Analytical expressions for these two possible scenarios have been proposed for vertical rods.[29,30] As an approximation for the torque level expected on our platelets, we use these expressions taking a rod diameter equivalent to the thickness (short-axis size) of our platelets.

For two vertical rods separated by a distance *d* and connected through an isolated meniscus bridge, the Laplace pressure ΔP and resulting torque $\vec{T}_{cap}$ that drives the rod from a vertical to a horizontal orientation is given by:[32,33]

$$T_{cap} = \frac{\pi \gamma L^3}{2\sqrt{d^2 - L^2}}, \quad \text{(Eq. S9)}$$

where γ is the surface tension of the liquid-air interface, *d* is the inter-particle distance as depicted in Fig. 1C, *L* is the particle height and β the angle of the meniscus on the particle surface.

In the partially immersed conditions, the bending torque resulting from the capillary forces is given by:[32,33]

$$T_{cap} = \frac{\gamma L^3}{d - L}. \quad \text{(Eq. S10)}$$

Experimental measurements of interparticle distances in a dried structure (Supplementary Figure 2) show that *d* varies between 12 µm and 100 nm, depending on the volume fraction of particles in the initial suspension. Taking the surface tension of water (γ = 0.073 N/m) and the size of the platelets (*L* = 8.9 µm), these *d* values can be used to estimate the range of capillary torques expected during drying. The torque calculated using the isolated meniscus bridge assumption (Eq. S9) ranges from $5.8 \cdot 10^{-9}$ to $1.7 \cdot 10^{-8}$ N.mm, whereas the lateral capillary forces arising in the partially immersed configuration (Eq. S10) give torques up to $1 \cdot 10^{-11}$ N.mm. These torque levels are 4 to 5 orders of magnitude higher than the torque of $3.8 \cdot 10^{-15}$ N.mm expected form gravity. Thus, our analysis indicates that the capillary torque applied by the moving air–water interface dictates the motion of the particles during drying and should be counteracted by opposing steric interactions to maintain the platelets in the orientation initially imposed by the external magnetic field.

Free volume and hydrodynamic volume of platelets

To ensure that platelets establish steric interactions that counteract capillary forces, the free volume in which the particle can rotate needs to be smaller than the hydrodynamics radius of the platelets (R_h). By definition, the hydrodynamic radius is the equivalent radius within which an individual particle is free to rotate. In terms of particle volume, the following condition needs therefore to be fulfilled to prevent the undesired effect of capillary forces during drying:

$$V_{free} < V_{hydro} \quad \text{(Eq. S11)}$$

where $V_{hydro} = \frac{4}{3}\pi R_h^3$. (Eq. S12)

The hydrodynamic radius (R_h) of a particle with long- and short-axis dimensions *L* and *l*, respectively, is given by:[34]

$$R_h = \frac{3L}{4\sqrt{1+\left(\frac{l}{L}\right)^2} + \frac{L}{l}\ln\left(\frac{l}{L} + \sqrt{1+\left(\frac{l}{L}\right)^2}\right) - \frac{l}{L}}. \quad \text{(Eq. S13)}$$

The free volume of a particle (V_{free}) expressed as the average volume available for a single particle to move in the suspension without interparticle steric interactions can be written as a function of the volume fraction of particles in suspension (ν) as:

$$V_{free} = \frac{V_p}{\nu} \quad \text{(Eq. S14)}$$

with $V_p = \frac{\pi}{4} \cdot L^2 \cdot l$ as the volume of a disc-shape platelet.

Thus, the dependence of the particle free volume on the particle geometry and on the volume fraction of the suspension can be expressed by the relation:

$$V_{free} = \frac{\pi \cdot L^2 \cdot l}{4\,\nu} \quad \text{(Eq. S15)}$$

Therefore, the volume fraction above which steric interactions are expected to occur (ν_{min}) can be estimated taking the critical condition: $V_{free} = V_{hydro}$. This leads to:

$$\nu_{min} = \frac{3\ L^2 \cdot l}{16\ R_h^3} . \quad \text{(Eq. S16)}$$

Using this equation, we find that $\nu_{min} = 16.8\ vol\%$ for the platelet dimensions used in this study.

Liquid crystalline domains

Our analysis of the minimum volume fraction (ν_{min}) above which steric interactions are expected is based on similar arguments put forward to explain the assembly of anisotropic particles into liquid crystalline domains. According to Onsager's theory,[23,24] packing entropic effects arising from a reduction in free particle volume are expected to occur when $nL^3 \sim 6.8$, where n is the number density of platelets and L the longest dimension of the particle. At this condition, nematic and isotropic phases are predicted to coexist. From this relation, the volume fraction (ν_{I-N}) at which colloidal particles of the same aspect ratio start to form liquid crystalline nematic phases is given by:

$$\nu_{I-N} = \frac{\pi n L^3}{4\frac{L}{l}} \quad \text{(Eq. S17)}$$

Applying this equation to our particles, we find that $\nu_{I-N} = 17\ \%$. This value is very close to the minimum volume fraction of particles (ν_{min} = 16.8 vol%) predicted above from particle free volume calculations. Considering that the polydispersity of our particles should broaden the volume fraction range where nematic and isotropic phases coexist,[32,33] these estimates are in good agreement with the lower limit of the optimum particle concentration window for the MASC process (ν = 20 vol%).

Apparent viscosity of suspensions

The dependence of the suspension viscosity on the volume fraction of platelets can be described by the Krieger–Dougherty relation[37]:

$$\eta_r = \frac{\eta}{\eta_{liq}} = (1 - \frac{v}{v_m})^{-Bv_m} \quad \text{(Eq. S18)}$$

where η_r is the relative viscosity, defined as the ratio between the viscosity of the suspension and the viscosity of the background liquid, v is the volume fraction of particles, v_m is the maximum volume fraction of particles and *B* is the Einstein coefficient[37]. For the platelets considered here, a v_m value of 40 vol% and a *B* value of 2 were experimentally obtained by fitting this relation to the measured suspension viscosity (Figure 2d).

Suspension reflectance as a function of platelet orientation

The normalized intensity of light reflected from the suspension (*I*) changes with the platelet's angle (ψ) as expected from Fresnel's law. For specular reflections, the face of a platelet reflects the light in a mirror-like manner, such that:

$$I(\psi) = a_0 + a_1 \cos(w\psi) + a_2 sin^{n}(w\psi) \quad \text{(Eq. S19)}$$

where a_0, a_1, a_2, and w are experimental constants. Experimental data points fitted with this equation (Figure 3a) showed a correlation coefficient of $R^2 = 0.95$.

Time required for platelet alignment

The time t_a required for the alignment of an individual platelet subjected to a rotating magnetic field *H* in a Newtonian fluid can be theoretically estimated by performing a torque balance at the edge of the platelet, as previously suggested in the literature.[20,21,38] For an applied frequency $\omega > \omega_c$, the platelets are not able to rotate with the imposed magnetic field and will thus biaxially align within the plane of the rotating field after an elapsed time t_a. In this work, we imposed the condition $\omega > \omega_c$ by applying a rotating frequency higher than the critical frequency as described by Erb et al.[20,21] As a result, our platelets behave in phase-ejected mode, as opposed to the phase-locked mode modelled in previous studies.[20,21]

Alignment of a phase-ejected platelet within the plane of the rotating magnetic field will still be driven by the magnetic torque T_m, which is counteracted by the viscous torque T_v. Assuming the viscosity of the fluid around a platelet to be high enough to dampen the rotation, the following force balance applies: $T_m = T_v$.

The magnetic torque T_m depends on the platelet orientation (Eq. S2), but also on the elasped time due to the rotation of the applied magnetic field (Supplementary Figure 1). To simplify the analysis we use an averaged torque, $\bar{T}_m$, in the force balance. This averaged torque is obtained by replacing the actual magnetic field in Eq. S2 by the orientation- and time-averaged fields $\bar{H}_{0,t}$ and $\bar{H}_{0,\theta}$:

$$\bar{H}_{0,t} = \bar{H}_{0,\theta} = \frac{2H_0}{\pi} \quad \text{(Eq. S20)}$$

We note that this averaging procedure is a refinement of previous estimates of the alignment time of platelets under phase-ejection mode.[38]

Introducing Eq. S20 in Eq. S2:

$$T_m = \frac{16\mu_0\chi_{ps}^2}{3\pi^2(\chi_{ps}+1)}\left[(a+d)(b+d)^2 - ab^2\right]H_0^2 \quad \text{(Eq. S21)}$$

Balancing the absolute values of the magnetic and viscous torques described in equations S3 and S21, we obtain the following relation:

$$dt = \frac{C_2}{H_0^2}d\theta \quad \text{(Eq. S22)}$$

where $C_2 = \frac{9\pi^2\eta V(f/f_0)(\chi_{ps}+1)}{8\mu_0\chi_{ps}^2\left[(a+d)(b+d)^2 - ab^2\right]}$

Integrating Eq. S22 on both sides for the intervals 0 < t < ta and 0 > θ > π/2, we arrive at:

$$t_a = \frac{C_1}{H_0^2}, \quad \text{(Eq. S23)}$$

where $C_1 = \frac{9\pi^3\eta V(f/f_0)(\chi_{ps}+1)}{16\mu_0\chi_{ps}^2\left[(a+d)(b+d)^2 - ab^2\right]}$.